JCB Article

Muscle-specific expression of insulin-like growth factor I counters muscle decline in *mdx* mice

Elisabeth R. Barton,[1] Linda Morris,[1] Antonio Musaro,[2] Nadia Rosenthal,[3] and H. Lee Sweeney[1]

[1]Department of Physiology, University of Pennsylvania, Philadelphia, PA 19104
[2]University of Rome "La Sapienza," Department of Histology and Medical Embryology, 00161 Roma, Italy
[3]Cardiovascular Research Center, Massachusetts General Hospital, Charlestown, MA 02129

Duchenne muscular dystrophy is an X-linked degenerative disorder of muscle caused by the absence of the protein dystrophin. A major consequence of muscular dystrophy is that the normal regenerative capacity of skeletal muscle cannot compensate for increased susceptibility to damage, leading to repetitive cycles of degeneration–regeneration and ultimately resulting in the replacement of muscle fibers with fibrotic tissue. Because insulin-like growth factor I (IGF-I) has been shown to enhance muscle regeneration and protein synthetic pathways, we asked whether high levels of muscle-specific expression of IGF-I in *mdx* muscle could preserve muscle function in the diseased state. In transgenic *mdx* mice expressing *mIgf-I* (*mdx:mIgf*$^{+/+}$), we showed that muscle mass increased by at least 40% leading to similar increases in force generation in extensor digitorum longus muscles compared with those from *mdx* mice. Diaphragms of transgenic *mdx:mIgf*$^{+/+}$ exhibited significant hypertrophy and hyperplasia at all ages observed. Furthermore, the IGF-I expression significantly reduced the amount of fibrosis normally observed in diaphragms from aged *mdx* mice. Decreased myonecrosis was also observed in diaphragms and quadriceps from *mdx:mIgf*$^{+/+}$ mice when compared with age-matched *mdx* animals. Finally, signaling pathways associated with muscle regeneration and protection against apoptosis were significantly elevated. These results suggest that a combination of promoting muscle regenerative capacity and preventing muscle necrosis could be an effective treatment for the secondary symptoms caused by the primary loss of dystrophin.

Introduction

The muscular dystrophies are degenerative disorders of muscle where there is marked muscle weakness and fragility. A subset of these diseases are caused by mutations in genes encoding proteins of the dystrophin-associated glycoprotein complex at the sarcolemma, and lead to its partial or complete absence (for review see Campbell, 1995). The most common form of the disease, affecting 1 out 3,500 newborn males, is Duchenne muscular dystrophy in which dystrophin is absent. Without the dystrophin complex to tether the actin cytoskeleton inside the muscle cell to the extracellular matrix, forces generated by the muscle fiber result in tears of the sarcolemma and lead to muscle damage. The regenerative capacity in muscle cannot compensate for increased susceptibility for structural damage. Therefore, a secondary consequence in dystrophic muscle is the inability of the muscle to adequately repair itself. The imbalance between muscle damage and muscle repair leads to a loss of muscle fibers and an increase in the amount of fibrosis over time until the functional capacity of the muscle diminishes to a point below the required force output.

Insulin-like growth factor I (IGF-I)* plays a critical role in muscle regeneration. It promotes the proliferation and differentiation of satellite cells in the muscle, enabling them to fuse to existing muscle fibers and repair damaged regions (Engert et al., 1996; for review see Florini et al., 1996). High and constant levels of IGF-I also cause significant muscle hypertrophy, which has been shown in numerous studies where IGF-I has been infused, introduced by recombinant virus, or overexpressed in transgenic animals (Adams and

Address correspondence to H. Lee Sweeney, Department of Physiology, B400 Richards Building, 3700 Hamilton Walk, University of Pennsylvania, Philadelphia, PA 19104. Tel.: (215) 898-8725. Fax.: (215) 573-2273. E-mail: lsweeney@mail.med.upenn.edu

N. Rosenthal's current address is EMBL Mouse Biology Programme, via Ramarini 32, 00016 Monterotondo, Roma, Italy.

Key words: IGF-I; muscular dystrophy; satellite cells; regeneration; protein kinase B

*Abbreviations used in this paper: EDL, extensor digitorum longus; HGF, hepatocyte growth factor; IGF-I, insulin-like growth factor I; Lo, optimum muscle length; *mdx:mIgf*$^{+/+}$, transgenic *mdx* mice expressing *mIgf-I*; *mIgf*$^{+/+}$, transgenic mice expressing *mIgf-I*; P-Akt, phosphorylated Akt; PI3K, phosphoinositol 3-kinase; PKB or Akt, protein kinase B.

Table I. **Animal and muscle masses in control, *mIgf*$^{+/+}$, *mdx*, and *mdx:mIgf*$^{+/+}$ mice**

Strain	Control	*mIgf*$^{+/+}$	*mdx*	*mdx:mIgf*$^{+/+}$
Muscle IGF-I (ng/g)	9 ± 1	16.2 ± 2[a]	8 ± 0	14 ± 1[a,b]
Body weight (g)	24.7 ± 0.1	35.5 ± 0.3[a]	33.1 ± 0.8[a]	40.0 ± 0.7[a,b]
Quadriceps (mg)	214.4 ± 8.7	312.7 ± 29.9[a]	291.7 ± 11.8[a]	380.4 ± 9.8[a,b]
Tibialis anterior (mg)	51.9 ± 0.9	74.1 ± 0.1[a]	79.6 ± 1.2[a]	114.2 ± 3.3[a,b]
EDL (mg)	10.2 ± 0.2	12.7 ± 0.5[a]	15.7 ± 0.4[a]	25.6 ± 0.5[a,b]
Soleus (mg)	9.2 ± 0.3	8.8 ± 0.5	14.9 ± 0.2[a]	14.8 ± 0.3[a]
Heart (mg)	128.4 ± 4.5	125.5 ± 2.2	126.8 ± 5.5	119 ± 7.8

Data represent mean ± SEM for muscles from four mice, aged 3 mo. Muscle IGF-I was determined from acetic acid extracts (D'Ercole et al., 1984) of limb muscle by Quest Diagnostics.
[a]Statistically significant compared to C57Bl/6 controls, $P < 0.05$.
[b]Statistically significant compared to *mdx* controls, $P < 0.05$.

McCue, 1998; Barton-Davis et al., 1998; Coleman et al., 1995; Lynch et al., 2001; Musaro et al., 2001). In addition, muscle enlargement in these animals results in an increased capacity of force generation. In aging-related declines in muscle mass and strength, it is thought that a significant factor is an impaired regenerative capacity (Barton-Davis et al., 1998; Musaro et al., 2001). IGF-I enhances regenerative capacity via the stimulation of satellite cell proliferation and differentiation. Furthermore, IGF-I promotes protein synthetic pathways (Russell-Jones et al., 1994; Adams and McCue, 1998), which can override muscle degeneration.

Because it is clear that IGF-I can prevent aging-related loss of muscle function (Barton-Davis et al., 1998; Renganathan et al., 1998), it is possible that IGF-I can prevent or diminish muscle loss associated with disease. Although the presence of IGF-I can do nothing for the primary defect in muscular dystrophy, it is possible that significant benefit might be derived from defending against the secondary symptoms associated with the disease. IGF-I could induce functional hypertrophy in muscle that is inherently weak. First, IGF-I could enhance muscle regenerative capacity to offset the imbalance between muscle damage and repair. Second, IGF-I could promote protein synthetic pathways and prevent muscle-wasting pathways. The combined effect of enhanced repair and decreased wasting might lead to greater functional capacity over time, where there is a reduction in the proportion of maximal effort needed to produce a required force, so the muscle is less likely to be damaged by normal activity.

Using the *mdx* mouse, a naturally occurring animal model for Duchenne muscular dystrophy (Sicinski et al., 1989), we asked if overexpression of IGF-I would promote muscle repair mechanisms and improve the dystrophic condition. Although not as severe as the *mdx:utr*$^{-/-}$ mouse (Deconinck et al., 1997), muscles from the *mdx* mouse exhibit critical hallmarks of the human form of the disease, including a high susceptibility to contractile-induced damage, a significant degree of muscle fiber degeneration and regeneration, and increased fibrosis later in life (Anderson et al., 1987; Carnwath and Shotton, 1987). The diaphragm of the *mdx* mouse, in particular, displays a Duchenne-like phenotype (Stedman et al., 1991). To introduce IGF-I into the *mdx* animals, we crossbred them with a recently characterized transgenic mouse that expresses high levels of IGF-I in muscle (Musaro et al., 2001). IGF-I transgene expression is restricted to muscle by using the myosin light chain 1/3 promoter; the mice exhibit significant muscle hypertrophy with no adverse side effects as well as enhanced regenerative capacity in aging muscle (Musaro et al., 2001). This approach allowed for the assessment of the maximum potential benefit that could be derived from IGF-I expression for dystrophic muscle, as well as examination of both the diaphragm and the extensor digitorum longus (EDL), which display a spectrum of dystrophic pathologies. By analyzing both muscle morphology and function in transgenic IGF/*mdx* crosses (transgenic *mdx* mice expressing *mIgf-I* [*mdx:mIgf*$^{+/+}$]), we observed significant improvement in muscle mass and strength, a decrease in myonecrosis, and a reduction in fibrosis in aged diaphragms.

Results

Morphology

A chemiluminescent assay was used to determine the amount of IGF-I in muscles from all strains. IGF-I content in muscles from transgenic mice expressing *mIgf-I* (*mIgf*$^{+/+}$ and *mdx:mIgf*$^{+/+}$) doubled compared with *mdx* and control animals (Table I). This level of IGF-I was sufficient to pro-

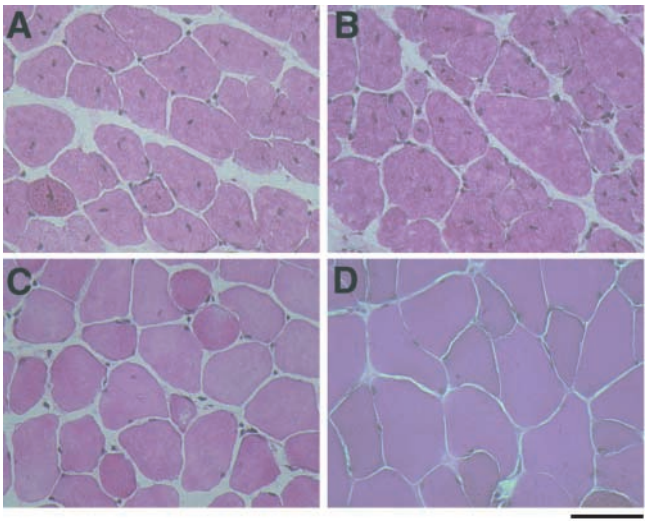

Figure 1. **Hemotoxilin and eosin histology of young (3 mo) EDLs.** Images reveal the fiber hypertrophy in both *mIgf*$^{+/+}$ strains, and that central nuclei remain in *mdx:mIgf*$^{+/+}$ in similar proportions to *mdx* muscle. (A) *mdx*; (B) *mdx:mIgf*$^{+/+}$; (C) control; (D) *mIgf*$^{+/+}$. Bar, 50 μm.

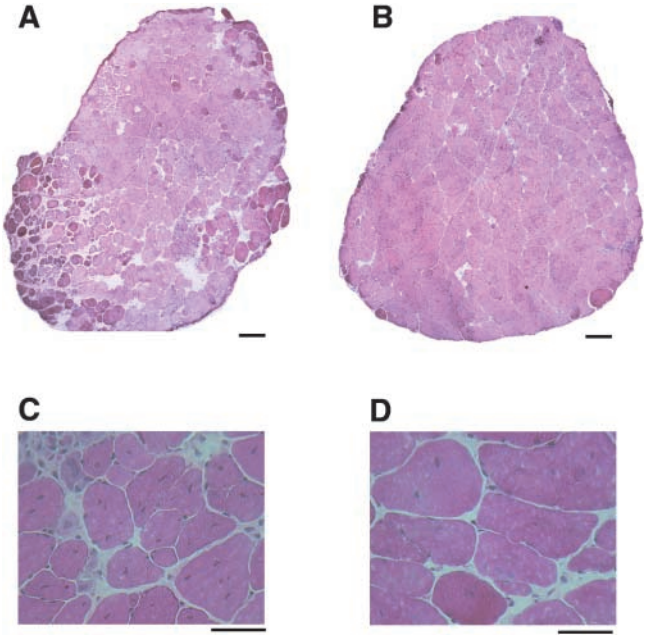

Figure 2. **Hemotoxilin and easin histology of aged (14 mo) EDLs.** *mdx* (A and C) and *mdx:mIgf*$^{+/+}$ (B and D) mice. Igf-I expression preserves *mdx* muscle homogeneity and promotes muscle hypertrophy. Bars: (A and B) 100 μm; (C and D) 50 μm.

mote increased muscle size in the transgenic animals. Muscles from *mdx* mice show significant hypertrophy when compared with nondystrophic muscles. The addition of muscle-specific IGF-I expression in *mdx* muscle caused significant hypertrophy over and above that normally found in these animals (Table I and Fig. 1). Muscle mass was increased by ~63% in EDL muscles from young *mdx:mIgf*$^{+/+}$ mice as compared with those from *mdx* mice, and was maintained at this level through at least 1 yr of age (Fig. 2). This hypertrophy was greater than that measured in the EDL muscles from the *mIgf*$^{+/+}$ animals, where there was a 40% increase in muscle mass compared with nontransgenic controls (Table I) (Musaro et al., 2001). Muscles that expressed the transgene at very low levels, as in the soleus, or did not express the transgene at all, such as the heart, displayed no significant hypertrophy when compared with nontransgenic *mdx* tissues (Table I).

EDL muscles were further analyzed to determine the source of the increased mass. A combination of hypertrophy of the muscle fibers and an increase in fiber number contributed to the higher weights of the EDLs from young *mdx:mIgf*$^{+/+}$ animals (Fig. 3, A and B). Fiber numbers followed the following trend: *mdx:mIgf*$^{+/+}$ > *mdx* > *IGF*$^{+/+}$ = con-

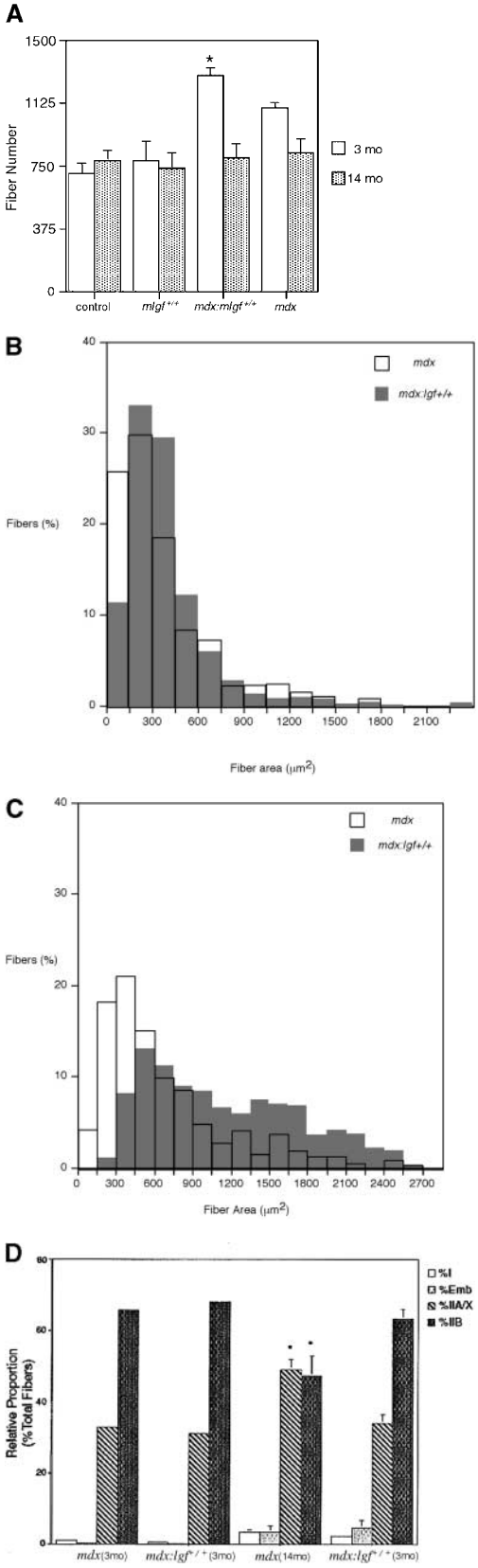

Figure 3. **Fiber analysis of EDL muscles.** (A) The number of fibers in the midbelly cross section of young EDL muscles was significantly higher in *mdx:mIgf*$^{+/+}$ muscles compared with *mdx* muscles. By 14 mo of age, however, the difference in fiber number disappeared. (B) Fiber size distribution in young EDL muscles. There was a rightward shift indicative of an increase in fiber area in young *mdx:mIgf*$^{+/+}$ muscles compared with *mdx* muscles. (C) Fiber size distribution in aged EDL muscles. The increase in fiber area was also observed in EDL muscles from 14-mo-old *mdx:mIgf*$^{+/+}$ animals. However, the distribution of fiber sizes in older muscles from both strains was significantly wider compared with younger muscles. (D) Fiber type distribution of *mdx* and *mdx:mIgf*$^{+/+}$ EDL muscles. Young EDL muscles displayed no shift in fiber type composition with IGF-I expression. However, the decline in the IIb fiber population associated with older *mdx* EDLs was prevented in EDLs from *mdx:mIgf*$^{+/+}$ mice. *, statistically significant from young *mdx* EDL, $P < 0.05$.

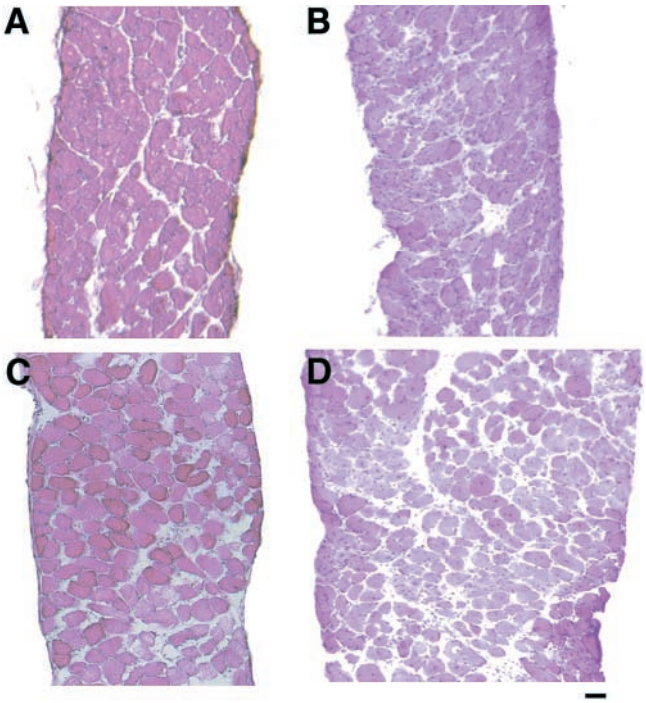

Figure 4. **Histology of young diaphragms from control, *mIgf*$^{+/+}$, *mdx*, and *mdx:mIgf*$^{+/+}$ mice.** Diaphragms from 3-mo-old *mdx:mIgf*$^{+/+}$ animals (D) were ~60% thicker than age-matched *mdx* control diaphragms (B). There was modest hypertrophy in young *mIgf*$^{+/+}$ diaphragms (C) compared with controls (A), but due only to increased fiber size not to an increase in fiber number.

trol. Therefore, IGF-I increased the hyperplasia normally observed in *mdx* muscle, an effect that differed from the response of control muscle to high levels of IGF-I. However, by 14 mo of age, the increase in fiber number in *mdx:mIgf*$^{+/+}$ EDL muscles disappeared, and the increased muscle size was solely due to hypertrophy of the muscle fibers (Fig. 3, A and C). Fiber type distribution, as assessed by immunostaining with antibodies recognizing types I, IIa, and IIb and embryonic myosin heavy chains, was not affected by IGF-I expression in young (3 mo old) EDL muscles. As *mdx* mice age, the continuous cycles of degeneration and regeneration lead to an increase in the heterogeneity of fiber size and a loss of fast fiber types (Anderson et al., 1987). An examination of 14-mo-old EDL muscles from *mdx:mIgf*$^{+/+}$ mice showed that the distribution of fiber type was preserved, compared with those from *mdx* animals (Fig. 3 D).

The EDL is an infrequently used muscle in a cage-reared mouse, and thus does not provide a rigorous test for the potential of IGF-I to counter dystrophin loss. The heavy demand on the mouse diaphragm makes it a more appropriate model for the human dystrophies especially in the *mdx* background. By 1 yr of age in the *mdx* mouse, the diaphragm displays dramatically increased fibrosis and functional loss (Stedman et al., 1991). Thus, the diaphragm was examined in 3- and 14-mo-old *mdx:mIgf*$^{+/+}$ mice. These results were more dramatic than those found in limb muscles. Young *mdx:mIgf*$^{+/+}$ diaphragms were significantly thicker than *mdx* controls, which was due to a combination of increased fiber size and number (Figs. 4 and 5). The number of fibers in the sagittal plane of the diaphragm significantly increased in young

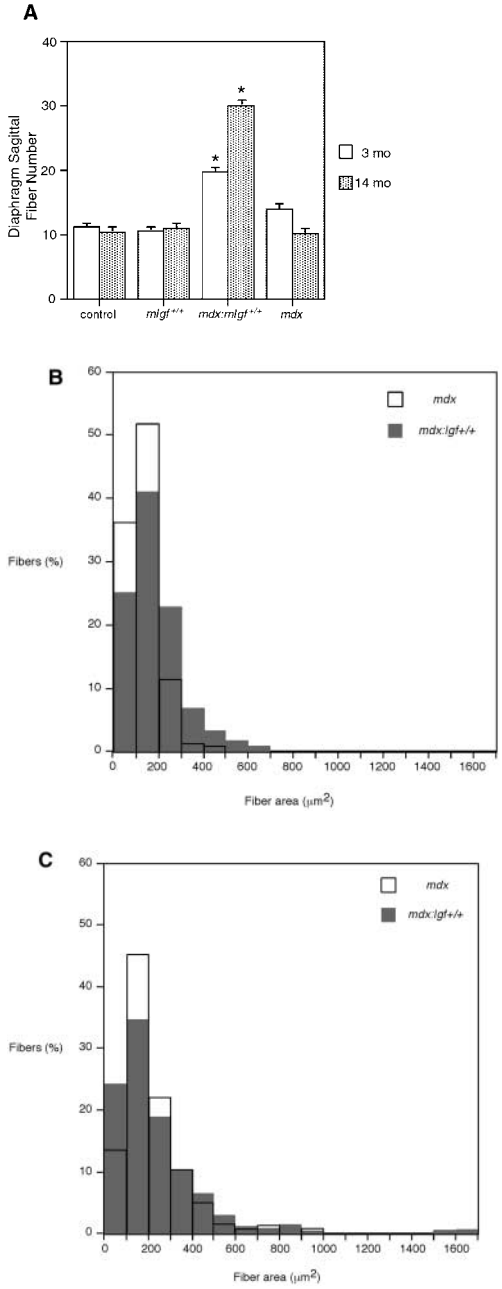

Figure 5. **Fiber analysis of diaphragms.** (A) The number of fibers across the sagittal plane of the *mdx:mIgf*$^{+/+}$ diaphragm was almost double that of other strains at 3 mo of age, and by 14 mo, there were approximately three times as many fibers when compared with age-matched diaphragms from the other mouse strains. (B) Fiber size increased in young *mdx:mIgf*$^{+/+}$ diaphragms as the proportion of larger fibers was greater than in *mdx* diaphragms. (C) By 14 mo, there was a leftward shift in fiber size distribution in the *mdx:mIgf*$^{+/+}$ diaphragms. Thus, the increased thickness of young *mdx:mIgf*$^{+/+}$ diaphragms was due to a combination of hyperplasia and fiber hypertrophy, whereas the increased size of aged *mdx:mIgf*$^{+/+}$ diaphragms was due primarily to hyperplasia. *, statistically significant from *mdx* diaphragm, $P < 0.05$.

mdx:mIgf$^{+/+}$ animals (Fig. 5 A). There was also an increase in fiber size, as shown by the rightward shift in the fiber size distribution (Fig. 5 B). The response to IGF-I was amplified in the diaphragms of old mice, which tripled in thickness when compared with diaphragms from *mdx* controls (Fig. 5 A and

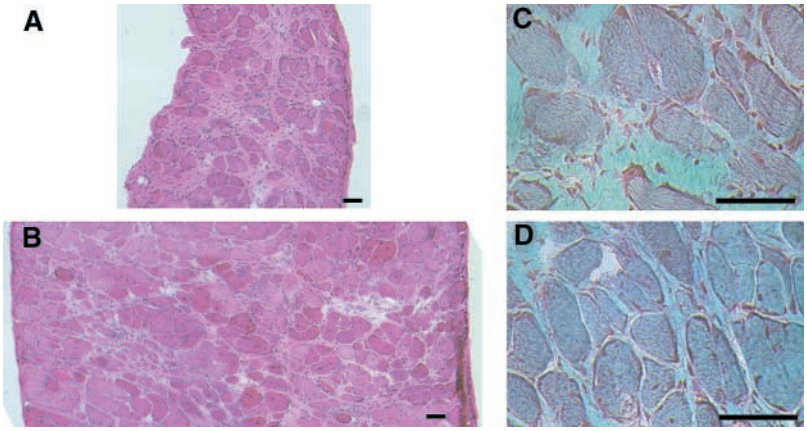

Figure 6. **Histology of aged (14 mo) diaphragms.** In 14-mo-old animals, the hypertrophic response continued; the thickness of *mdx:mIgf*$^{+/+}$ diaphragms (B) were triple that of *mdx* controls (A). Gomori's trichrome staining (C and D) revealed a reduction in connective tissue in *mdx:mIgf*$^{+/+}$ diaphragms (D) compared with those from *mdx* controls (C). Bars, 50 μm.

Fig. 6). In contrast to the young diaphragms, hyperplasia was the primary source for the increased size in the *mdx:mIgf*$^{+/+}$ diaphragms (Fig. 5 A), as there was no rightward shift in fiber size distribution (Fig. 5 C).

One of the hallmark symptoms of muscular dystrophy is increased fibrosis later in life. We used Gomori trichrome staining and hydroxyproline measurements to assess the level of fibrosis in 14-mo-old diaphragms. The replacement of muscle fibers by fibrotic tissue was prevented by IGF-I expression. In aged diaphragms, collagen content was maintained at normal levels (Fig. 6, C and D, and Fig. 7).

Functional analysis

Even though dystrophic muscles are larger than normal healthy muscles, the increased muscle mass has impaired strength due to a reduction in the force per cross-sectional area (specific force). Analysis of the force-generating capacity in the EDLs from young *mdx:mIgf*$^{+/+}$ animals showed that the increase in muscle size produced a proportional increase in force, although the specific force was uncorrected (Table II). The cross-sectional area (Brooks and Faulkner, 1988) of EDL muscles from *mdx:mIgf*$^{+/+}$ animals was 49 ± 6% greater than nontransgenic *mdx* EDLs. A comparable increase in tetanic force was also observed; transgenic EDLs generated 37± 16% more force than muscles from nontransgenic animals. This trend held in aged EDLs, where muscle hypertrophy and comparable increases in muscle force were also observed. The specific force of these muscles, however, was similar to that of dystrophic muscles (Table II). Thus the *mdx:mIgf*$^{+/+}$ muscle increases functional capacity by increasing muscle mass, but not by increasing specific force.

It is possible that this increase in the absolute force–generating capacity of the *mdx:mIgf*$^{+/+}$ muscles affords protection against contractile damage, because less muscle mass will be needed to produce a given amount of force and work. Thus, either the number of fibers recruited and/or the recruitment frequency may be lower in the *mdx:mIgf*$^{+/+}$ as compared with either *mdx* or normal muscle. This is illustrated in Fig. 8. The maximum force generated by *mdx* or C57 EDLs at 120 Hz, which was the fusion frequency under our conditions, is comparable to the force generated in *mdx:mIgf*$^{+/+}$ muscles stimulated at only 70–80 Hz (Fig. 8 A, dotted line). Reduced relative load on the muscle may result in less damage being incurred during routine use of the muscles. To demonstrate that this is the case for the *mdx:mIgf*$^{+/+}$ cross, eccentric contractions were performed at equivalent forces (*mdx:mIgf*$^{+/+}$ at 80 Hz vs. *mdx* and C57 at 120 Hz) and equivalent recruitment frequencies (80 Hz for all strains). The results of this experiment are shown in Fig. 8 B. The decrement of force between the first and fifth contractions in muscles from *mdx* and *mdx:mIgf*$^{+/+}$ animals was similar at equivalent stimulation frequencies (34.5 ± 9.8% vs. 37.3 ± 8.7% for *mdx* and *mdx:mIgf*$^{+/+}$, respectively). However, when muscles were subjected to eccentric contractions at equivalent forces (Fig. 8 B, right), *mdx* muscles experienced significantly greater drops in force (37.3 ± 8.7% for *mdx:mIgf*$^{+/+}$ at 80 Hz vs. 64.3 ± 3.4% for *mdx* at 120 Hz). Muscles from C57 animals incurred minimal damage at either stimulation frequency (Fig. 8 B). Thus, although susceptibility to contractile damage is still present in *mdx:mIgf*$^{+/+}$ muscles, the fact that a reduced proportion of the transgenic muscle is required for the generation of equivalent force, compared with *mdx* muscles, reduces the potential for damage.

Further evidence for a reduction of myonecrosis in *mdx:mIgf*$^{+/+}$ animals is found in muscles from Evan's blue dye–injected mice (Fig. 9) (Straub et al., 1997). Both the quadriceps and the diaphragm from *mdx:mIgf*$^{+/+}$ animals show significantly less dye uptake than the same muscles from *mdx* animals. As an indicator of whole animal muscle damage,

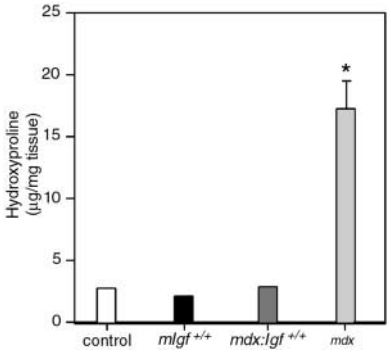

Figure 7. **Hydroxyproline content of aged diaphragm muscles.** Hydroxyproline levels, an index of fibrosis, were reduced in 14-mo-old *mdx:mIgf*$^{+/+}$ diaphragms to normal levels found in age-matched *mIgf*$^{+/+}$ and control muscles. Measurements were performed in duplicate on $n = 2$ muscle samples from each mouse strain. *, statistically significant ($P < 0.05$) from age-matched control diaphragm.

Table II. **Contractile properties of EDL muscles from 3-mo-old mice**

Strain	Control	*mIgf*$^{+/+}$	*mdx*	*mdx:mIgf*$^{+/+}$
Cross-sectional area (mm^2)	1.93 ± 0.05	2.33 ± 0.01[a]	2.27 ± 0.06[a]	3.38 ± 0.06[a,b]
Tetanic force (mN)	406.3 ± 16.7	595 ± 6.5[a]	352 ± 20[a]	482 ± 26[a,b]
Specific force (N/cm^2)	21.0 ± 0.8	25.5 ± 0.3[a]	15.4 ± 0.7[a]	14.3 ± 0.8[a]

Data represent mean ± SEM for muscles from four mice for each strain. Cross-sectional area was determined using the methods of Brooks and Faulkner (1988).
[a]Statistically significant compared to C57Bl/6 controls, $P < 0.05$.
[b]Statistically significant compared to mdx controls, $P < 0.05$.

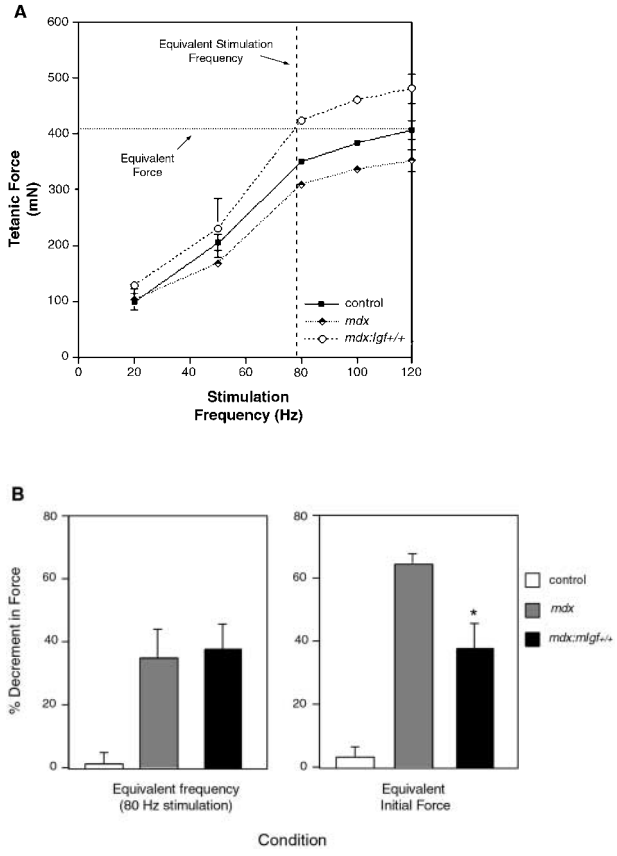

Figure 8. **Functional assessment of EDLs from *mdx* and *mdx:mIgf*$^{+/+}$ mice.** (A) Force frequency relationship of EDL muscles. The maximum force generated by control and *mdx* EDLs at 120 Hz is comparable to the force generated in *mdx:mIgf*$^{+/+}$ muscles stimulated at ~70–80 Hz (dotted line). Eccentric contractions were performed at equivalent forces (*mdx:mIgf*$^{+/+}$ at 80 Hz vs. *mdx* and control at 120 Hz) and at equivalent stimulation frequencies (dashed line, 80 Hz for all strains). (B) Damage associated with eccentric contractions in *mdx*, *mdx:mIgf*$^{+/+}$, and control EDLs. (B, left) EDL muscles were subjected to five eccentric contractions with a 10% Lo stretch during stimulation at 80 Hz. The decrement of force between the first and last contraction is not significantly different between *mdx* and *mdx:mIgf*$^{+/+}$ muscle at this stimulation frequency (34.5 ± 9.8% vs. 37.3 ± 8.7% for *mdx* and *mdx:mIgf*$^{+/+}$, respectively), and both are more susceptible to damage than control muscles. (B, right) When muscles were subjected to eccentric contractions at equivalent force, *mdx* muscles experienced significantly greater drops in force (37.3 ± 8.7% for *mdx:mIgf*$^{+/+}$ at 80 Hz vs. 64.3 ± 3.4% for *mdx* at 120 Hz, $P < 0.05$). Control muscles were not susceptible to contraction-induced injury at 120-Hz stimulation frequency. *, statistically significant ($P < 0.05$) from age-matched *mdx* muscles.

serum creatine kinase measurements were performed on 3-mo-old animals. There is a 40% decrease in serum creatine kinase levels in *mdx:mIgf*$^{+/+}$ animals compared with *mdx* controls (472 ± 60 U/L vs. 839 ± 121 U/L, respectively, for $n = 6$ mice), and these levels are indicative of a reduction in contractile damage for the whole animal.

Activation of Akt

Protein kinase B (PKB or Akt) activation has been shown to be a major component of how IGF-I mediates cell survival and growth in muscle (Alessi and Cohen, 1998; Lawlor and Rotwein, 2000a; Wu et al., 2000). To examine if IGF-I activated this pathway in the transgenic animals, we measured the level of Akt phosphorylation as an indicator of pathway activation. Results of these measurements are shown in Fig. 10. Akt phosphorylation was dramatically higher in *mdx:mIgf*$^{+/+}$ muscle compared with all other strains studied. Total Akt protein was modestly higher in *mdx, mIgf*$^{+/+}$, and *mdx:mIgf*$^{+/+}$ compared with wild-type muscle, but not high enough to account for the increase in Akt activation. Surprisingly, Akt phosphorylation in *mIgf*$^{+/+}$ muscle did not differ from control tissue. However in *mdx:mIgf*$^{+/+}$ muscle, the drive for regeneration remains high throughout the life of the animal, and the pathways by which fiber regeneration is regulated, including the phosphoinositol 3-kinase (PI3K)/Akt pathway, also remain active.

An additional contribution to the improved status of *mdx:mIgf*$^{+/+}$ muscle may arise from the anti-apoptotic properties of IGF-I (Lawlor and Rotwein, 2000a,b). These effects have been shown to be mediated via the PI3K pathway (involving Akt activation) in a number of cell types, including muscle (Lawlor and Rotwein, 2000b; Wu et al., 2000). A heightened level of apoptosis has been observed in *mdx* muscle, possibly due to calcium overload from sarcolemmal damage or perforin-mediated cytotoxicity (Spencer et al., 1997; Sandri et al., 1998; Sandri and Carraro, 1999). Although we observed a low level of apoptosis in *mdx* muscles (<0.5%; unpublished data), the dynamic range between normal and dystrophic tissue was too small to enable direct detection of any anti-apoptotic effect of IGF-I in *mdx:mIgf*$^{+/+}$ animals. However, there is the clear potential to enhance protection against apoptosis via increased Akt activation.

Discussion

The major findings of this study all indicate that muscle-specific expression of IGF-I can counter aspects of the muscular dystrophy associated with the loss of dystrophin. The effects

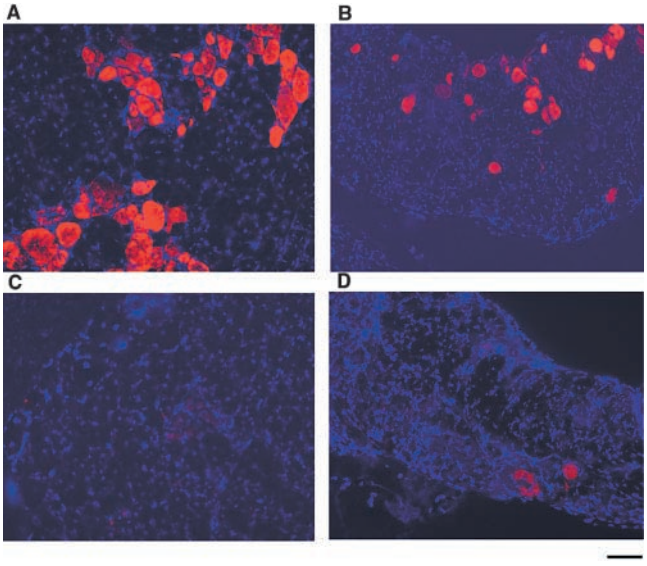

Figure 9. **Evan's blue staining on cryosections from young (3 mo) *mdx* and *mdx:mIgf*$^{+/+}$ muscles.** 10-μm cryosections from *mdx* (A and B) and *mdx:mIgf*$^{+/+}$ (C and D) mice. Quadriceps (A and C) and diaphragms (B and D). Bar, 100 μm.

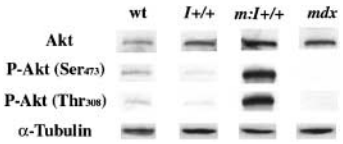

Figure 10. **Immunoblot analysis of total Akt, P-Akt, and α-tubulin in quadriceps muscles from 3-mo-old control (wt), *mIgf*$^{+/+}$, *mdx*, and *mdx:mIgf*$^{+/+}$ mice.** Akt phosphorylation of both serine 473 and threonine 308 was significantly amplified in *mdx:mIgf*$^{+/+}$ muscle, without a commensurate change in total Akt levels compared with muscles from *mIgf*$^{+/+}$ and *mdx* strains. Immunoblotting for α-tubulin served as a control for protein loading.

of IGF-I result in muscle hypertrophy, increased muscle strength (albeit with low specific force), decreased myonecrosis, and reduced muscle fibrosis. In contrast to the effects of IGF-I in transgenic mice, where expression of IGF-I regulated by a different muscle-specific promoter resulted in cardiac hypertrophy and elevated plasma levels of IGF-I (Delaughter et al., 1999), we did not see any deleterious effects on the heart. This is most likely due to the lower levels of IGF-I produced by the myosin light chain 1/3 promoter construct. There is ~20 times more IGF-I protein in the transgenic lines previously described (Coolican et al., 1997). This suggests that a small increase in local IGF-I production is sufficient to drive muscle hypertrophy. As we previously showed (Barton-Davis et al., 1998; Musaro et al., 2001), the IGF-I levels in the blood were not elevated and there was no effect seen in muscles that did not express the transgene. Furthermore, the affected muscles were not only hypertrophied, but maintained a uniformity of fiber size and type distribution, compared with muscles from *mdx* animals (Fig. 4). We propose that long-term IGF-I expression results in IGF-I–driven enhancement of the repair mechanisms that direct satellite cell activation, proliferation, and differentiation so that fiber degeneration does not go unchecked.

IGF-I is a potent signal for growth in a number of tissues. Limiting its expression to muscle by driving it with a fast muscle-specific promoter and using an isoform that does not enter the circulation enables skeletal muscle to be the sole target of IGF-I activity (Musaro et al., 2001). However, because skeletal muscle is comprised of multiple cell types, IGF-I secreted from muscle fibers could stimulate other cells in addition to muscle fibers and satellite cells. Fibroblasts, in particular, are responsive to IGF-I (Petley et al., 1999) and are the source of the increased collagen deposition seen in dystrophic muscles. In the transgenic mouse that overexpresses human IGF-I, fibrosis was observed in the heart in animals over 1 yr of age (Delaughter et al., 1999), confirming the possibility that in our model, IGF-I would drive fibrosis as well. Even though IGF-I has been shown to stimulate fibroblasts, there is a net decrease in fibrosis in diaphragms of the *mdx:mIgf*$^{+/+}$ mice. In fact, age-related fibrosis in the *mdx* diaphragm was effectively eliminated by IGF-I expression (Figs. 6 and 7). It may be that the efficient and rapid repair of the *mdx:mIgf*$^{+/+}$ muscles prevents the establishment of an environment into which the fibroblasts migrate. This is of particular relevance to the human dystrophic condition where virtually all skeletal muscles succumb to fibrosis (Louboutin et al., 1993; Morrison et al., 2000). Thus, the results found in the mouse diaphragm suggest that IGF-I might be effective not only in increasing muscle mass and strength, but also in reducing fibrosis associated with the disease.

The effect of IGF-I on other tissues might also contribute to the preservation of fiber type in the older animals. When muscle fibers are severely damaged and lose innervation, it has been shown that slow motor neurons are more apt to reinnervate the regenerated fibers (Desypris and Parry, 1990). Given that neurons also respond to IGF-I, it is possible that the difference in reinnervation properties is minimized in these animals. Alternatively, the muscle repair mechanisms, which are enhanced by the presence of IGF-I (Musaro et al., 2001), might aid in muscle repair without the occurrence of degeneration. Although we have not directly tested these possibilities, the lower degree of myonecrosis apparent in *mdx:mIgf*$^{+/+}$ muscle shows that there is less degeneration, and so perhaps less denervation. However, this observation does not exclude the potential effect on motor neurons.

The aged *mdx* diaphragm normally demonstrates a marked loss of fiber number (Stedman et al., 1991). However, in the aged *mdx:mIgf*$^{+/+}$ diaphragms, profound hyperplasia was observed. This suggests that the satellite cell pool in dystrophic tissue is not depleted over time, but instead, the signals that activate the regeneration diminish. With sufficient stimulation by exogenous IGF-I, the satellite cell proliferation more than compensates for the need for fiber regeneration. In normal muscle, the replicative capacity of satellite cells is sufficient to maintain muscle mass as long as existing muscle fibers can generate the appropriate signals for activating them (Allen et al., 1995; Chakravarthy et al., 2000a). With aging, we and others have proposed that the limiting factor in muscle regeneration is the availability of

growth and repair-inducing growth factors, including IGF-I and hepatocyte growth factor (HGF) (Barton-Davis et al., 1998; Chakravarthy et al., 2000b; Musaro et al., 2001). Satellite cells extracted from aged muscle can still respond to these factors if they are provided (Allen et al., 1995; Chakravarthy et al., 2000a). However, it is unclear what the limiting factor is in dystrophic muscle. Studies have shown that the mitotic potential of satellite cells from young muscular dystrophy patients is comparable to that found in human senescence, suggesting that the heightened necessity for muscle repair associated with muscular dystrophy could eventually deplete the pool of satellite cells (Decary et al., 2000). Although we have not examined muscles from extremely old *mdx:mIgf*$^{+/+}$ mice at this time, the observations of the 14-mo-old diaphragms support the hypothesis that the satellite cell pool is not depleted in dystrophic muscle and readily responds to increased levels of IGF-I.

Telomere length proves to be an excellent indicator of the number of divisions that a group of cells has undergone (Harley, 1997; Wright and Shay, 2000). A number of studies have shown that telomere length in human dystrophic muscle is significantly reduced compared with samples from healthy muscle (Decary et al., 1997, 2000). In mice, however, the number of base pairs lost per division is minimized by telomerase activity, which tends to maintain telomere length even after several divisions, thereby obscuring the correlation between replicative age and telomere length (Prowse and Greider, 1995; Wright and Shay, 2000). Therefore, although telomere length could provide some measure of whether IGF-I is depleting a satellite pool by driving proliferation, this question cannot be pursued in the mouse. If, however, IGF-I treatment is to become a reality in human disease, it will be essential to address this issue.

The effect of IGF-I on fiber number in *mdx* mice differs from the effect in normal mice. Under healthy conditions, activated satellite cells proliferate and fuse to existing fibers, or in the case of a damaged fiber, fuse to each other to form a new fiber within the basal lamina of the old one. In pathologic conditions, such as muscular dystrophy, perhaps the increased drive for satellite cell activation results in increased numbers of fibers, as has been shown in culture (Engert et al., 1996). Hyperplasia in the *mdx:mIgf*$^{+/+}$ muscles was exacerbated, particularly in the diaphragm (Figs. 4 and 6). This suggests that there may be some threshold level of satellite cell activation and/or muscle damage beyond which stimulated satellite cells begin to fuse with each other and form new fibers, in addition to fusing to existing damaged fibers.

It is unclear which factors involved in the proliferation and differentiation of satellite cells drive the regenerative process toward new fiber formation. Because IGF-I can regulate both processes, the levels or activation of additional factors that affect the ultimate outcome of the signaling pathways likely differ in *mdx* muscle. Possible factors include HGF, fibroblast growth factor, and myostatin, a muscle-specific member of the TGF-β superfamily (McPherron et al., 1997). Myostatin has been shown to block myoblast proliferation in vitro (Thomas et al., 2000), whereas HGF and fibroblast growth factor are involved in the activation and proliferation of satellite cells (Sheehan and Allen, 1999). Muscles from myostatin-null mice exhibit an increase in fiber size and number (McPherron et al., 1997). Thus, a change in the activation levels of any of these factors could contribute to the modest hyperplasia seen in the *mdx* mice, and, in combination with IGF-I, may contribute to the profound hypertrophy in the *mdx:mIgf*$^{+/+}$ mice. Other investigators have shown that, in muscle, activation of the MAPK cascade leads to the proliferation of cells (Coolican et al., 1997; Samuel et al., 1999). Therefore, the interaction of other factors with this arm of IGF-I activation would result in the differing effects of IGF-I in normal and dystrophic muscle. Either a reduction in the inhibition or an enhancement of activation of the MAPK pathway could lead to a greater proliferative response in the *mdx:mIgf*$^{+/+}$ cross as compared with the *mdx* only or the *mIgf*$^{+/+}$ animals. Although we have not examined the interactions between IGF-I and other growth factors in normal or dystrophic muscle at this time, these animals could serve as ideal models for studying the intracellular responses to these growth factors.

IGF-I also promotes cell survival, primarily through the PI3K pathway and Akt activation (Alessi and Cohen, 1998; Lawlor and Rotwein, 2000b). Cell culture studies have confirmed that the presence of IGF-I drives the PI3K pathway, particularly at the inception of differentiation (Musaro and Rosenthal, 1999; Chakravarthy et al., 2000a). Because heightened levels of apoptosis have been documented in dystrophic muscle (Spencer et al., 1997; Sandri et al., 1998; Sandri and Carraro, 1999), the activation of cell survival pathways during the regenerative process might provide some protection against cell death. Alternatively, amplified Akt phosphorylation in *mdx:mIgf*$^{+/+}$ muscle might only be reflective of the increased drive for fiber regeneration and differentiation. Recent work has identified Akt1 (PKBα) as the predominant isoform involved in cell survival, and Akt2 (PKBβ) as the primary player in differentiation (Vandromme et al., 2001). In this study, no distinction was made between the amount of phosphorylation of specific Akt isoforms. We can conclude that cell survival pathways are indeed heightened in *mdx:mIgf*$^{+/+}$ muscle. Further measurements are necessary to examine the Akt2/differentiation pathway.

One of the major consequences of the loss of dystrophin in muscle is a high susceptibility to contractile damage. As stated previously, IGF-I can do nothing directly to prevent this. However, the combined effect of increased strength and enhanced repair can indirectly counteract contractile damage. This might lead to greater functional capacity over time and extend the period during which dystrophic muscle is functional. There is a reduction in the proportion of maximal effort needed to produce a required force, so the muscle is less likely to be damaged by normal activity. The most damaging type of activity is eccentric contraction, where there is a very high strain imposed on the connections between the extracellular matrix and the cytoskeleton. In our experiments, assessment of the amount of damage incurred by eccentric contraction shows that *mdx:mIgf*$^{+/+}$ EDL muscles are just as susceptible to damage as muscles from *mdx* mice, but only when they are stimulated to achieve equivalent strain (same stimulation frequency). The more critical observation in this case is the comparison of contractile damage incurred at equivalent forces. As shown if Fig. 8, having greater functional muscle mass affords some protection

against damage when generating a given level of force. The benefit of more muscle in the *mdx:mIgf*$^{+/+}$ mice is also supported by the 40% reduction in serum creatine kinase levels.

Increased myofiber degeneration and necrosis is associated with many of the muscular dystrophies. We have observed a marked decrease in myonecrosis by Evan's blue staining in muscles from the *mdx:mIgf*$^{+/+}$ animals (Fig. 9), as well as a decrease in serum creatine kinase levels. These results suggest that IGF-I is promoting growth pathways sufficiently to offset the normal damage that is found in *mdx* muscle. Certainly, the increased phosphorylated Akt (P-Akt) levels serve as indicators for increased growth and survival. In addition to promoting growth pathways, enhanced regeneration caused by IGF-I (Musaro et al., 2001) acts in a complementary manner by repairing existing damage. These results show that on the whole animal level, IGF-I–driven functional hypertrophy of dystrophic muscle has therapeutic promise.

In summary, dystrophic muscles display a high susceptibility to contractile damage, increased cycles of degeneration and regeneration, a progressive decline in strength, and increased fibrosis later in life. The therapies being contemplated to treat the disease are generally directed at correction of the primary defect, the loss of dystrophin (Hartigan-O'Connor and Chamberlain, 2000; Rando et al., 2000; Wang et al., 2000). However, the sheer size of the dystrophin cDNA and the need to deliver the cDNA to all muscle cells throughout the body limit the ability of gene therapy techniques used for dystrophin replacement. An alternative strategy is to treat the secondary symptoms of the disease using a secreted growth factor that would have its effect on all of the fibers of a muscle, even if only a subset of the fibers received gene transfer. Through a number of different studies of normal muscle, IGF-I has been shown to be effective in increasing muscle mass and strength, promoting muscle regeneration, and preventing apoptosis (Barton-Davis et al., 1998; Chakravarthy et al., 2000a; Lawlor and Rotwein, 2000b; Lynch et al., 2001; Musaro et al., 2001). The results described here show that muscle-specific IGF-I expression is beneficial to dystrophic muscle, and, surprisingly, prevents fibrosis in addition to promoting functional hypertrophy. Thus, increasing the rate of muscle regeneration may be a therapeutic alternative to replacing the missing or defective dystrophin complex member in the dystrophinopathies (Duchenne, Becker, and a subset of Limb Girdle muscular dystrophies).

Materials and methods

Generation of transgenic animals

IGF transgenic male mice (*mIgf*$^{+/+}$) (Musaro et al., 2001) were bred with *mdx* female mice, resulting in a hemizygous F1 generation. Males and females from this generation were bred, resulting in a group of mice homozygous for the IGF-I gene and the X-linked *mdx* mutation. Mice were screened for the presence of both genes using previously described methods (Shrager et al., 1992; Barton-Davis et al., 1998; Musaro et al., 2001). The F2 generation had the expected proportions of homozygosity according to Mendelian genetics. Mice exhibiting the desired genotype were bred to establish homozygotic lines of *mdx:mIgf*$^{+/+}$ mice. Mice from the F4 and subsequent generations were used for analysis.

Muscle morphology

EDL muscles and sections of the anterolateral costal diaphragm were removed from 3- and 14-mo-old *mdx:mIgf*$^{+/+}$, *mIgf*$^{+/+}$, *mdx*, and C57Bl/6 (control strain) animals. All muscles were blotted and rapidly frozen in melting isopentane. EDL muscles were weighed before freezing. 10-μm frozen cross sections taken from the midbelly of the EDLs, and the midsection of the diaphragms (between the central tendon and ribcage) were stained with hematoxylin and eosin and Gomori's trichrome. Stained sections were visualized on a Leica DMR microscope and captured with a digital camera using image analysis software (OpenLab). Analysis of fiber number and size was performed on adjacent sections that had been immunostained for collagen IV (Chemicon International, Inc.) using the same image analysis software. The fiber numbers at the midbelly of the EDL were used for comparisons between animals. Fiber numbers across the sagittal plane of the diaphragms were used as an index of total fiber number. Fiber areas were assessed in a region containing ~500 fibers at the EDL midbelly and in 500 fibers in each diaphragm. Preliminary measurements confirmed that there was no significant difference between analysis of 500 fibers in a cross section and that of the entire cross section. Before morphological analysis, EDL muscles from young mice were analyzed for functional performance as described below. Total cross-sectional area (CSA) of EDL muscles was determined using the wet weight and optimum muscle length (Lo) found during functional assessment in the formula CSA (mm^2) = muscle mass (mg)/(fiber length/Lo) × (Lo[mm]) × 1.06 mg/mm^3), where fiber length/Lo = 0.45 (Brooks and Faulkner, 1988).

Muscle mechanical measurements

Isolated whole muscle mechanics was performed on EDL muscles from 3-mo-old *mdx:mIgf*$^{+/+}$, *mIgf*$^{+/+}$, *mdx*, and control animals using a previously described apparatus (Barton-Davis et al., 1998). Lo was defined as the length that produced maximum twitch tension. Maximum tetanic force at Lo was measured using a 120 Hz, 500-ms pulse at supramaximal voltage. Protection against mechanical injury was evaluated by inducing a series of five eccentric tetanic contractions. These were performed using a 700-ms stimulation period during which the muscle was held in an isometric contraction for the first 500 ms followed by a stretch of 10% Lo at a rate of 0.5 Lo/s. Protection against mechanical injury was evaluated at both 80- and 120-Hz stimulation frequencies. Damage was determined as the loss in force between the first and last eccentric contraction. At the end of the mechanical measurements, muscles were blotted, weighed, and then rapidly frozen in melting isopentane for subsequent histological analysis as described above.

Collagen content

Measures of hydroxyproline were used to assess the amount of fibrosis in the diaphragms of control, *mIgf*$^{+/+}$, *mdx*, and *mdx:mIgf*$^{+/+}$ mice at 14 mo of age (Amino Acid Analysis). Hydroxyproline content was normalized to tissue weight for comparisons among muscle samples.

Fiber type composition

Immunohistochemistry was used to determine myosin heavy chain composition (Schiaffino and Salviati, 1997). Primary antibody dilutions were as follows: type I myosin (BA-F8), 1:50; type IIa myosin (SC-71), 1:10; type IIb myosin (BF-F3), 1:3; embryonic myosin (BF-45), 1:50. FITC-conjugated goat anti–mouse IgM antibodies and donkey anti–mouse IgG (H + L) (Jackson ImmunoResearch Laboratories) were used as secondary antibodies. Microscopy was performed on a Leitz DMR microscope (Leica). Image acquisition and analysis were performed using a MicroMAX digital camera system (Princeton Instruments, Inc.) and imaging software (OpenLab).

Evan's blue staining

Evan's blue was injected into the tail vein of 3-mo-old *mdx:mIgf*$^{+/+}$, and *mdx* animals after the procedures previously described (Straub et al. 1997). Animals were killed 8 h after injection, and muscles were removed and rapidly frozen in melting isopentane. 10-μm frozen sections were fixed in cold acetone, rinsed in PBS, and covered with aqueous mounting media containing DAPI nuclear stain (Vectashield; Vector Laboratories). Image acquisition and analysis were performed as described in the fiber type composition methodology section.

Immunoblot analysis

Quantification of total Akt, P-Akt, and α-tubulin were determined by Western blotting. Quadriceps muscles from 3-mo-old animals were homogenized in 10 vol/muscle wet weight of modified lysis buffer (50 mM Tris-HCl, pH 7.4, 1% wt/vol Triton X-100, 0.25% sodium deoxycholate, 150 mM sodium chloride, 1 mM phenylmethylsulfonyl fluoride, 1 μg/ml aprotinin, 1 μg/ml leupeptin, 1 μg/ml pepstatin, 1 mM sodium orthovanadate, 1 mM sodium fluoride, 1 mM EGTA). Homogenates were centrifuged to pellet debris, and the total protein was measured in the supernatant (Bio-Rad Laboratories). Equal amounts of protein from each muscle lysate were

separated by 12% SDS-PAGE and transferred to polyvinylidene fluoride membranes (Immobilon-P; Millipore). Membranes were incubated in a blocking buffer (Tris-buffered saline plus 0.1% Tween 20 that contains 5% nonfat dry milk [5% milk–TTBS]) and then incubated in primary antibody diluted in 5% milk–TTBS overnight at 4°C. Membranes were then washed in 5% milk–TTBS and incubated with HRP-conjugated secondary antibody. After a series of washes in 5% milk–TTBS, TTBS, and TBS, protein detection was performed using ECL and exposure to X-ray film. Analysis of band intensity was performed using image analysis software (Kodak 1D; Eastman Kodak Co.) on the scanned films. Membranes were stained with Coomassie brilliant blue R-250 after immunoblotting to confirm equal protein loading. Antibodies and the conditions used in these measurements were as follows: rabbit anti–phospho-Akt (Ser473), 1:700 (Cell Signaling Technology); rabbit anti–phospho-Akt (Thr308), 1:700 (Cell Signaling Technology); sheep anti-Akt1, 1:300 (Upstate Biotechnology); HRP–anti-rabbit, 1:2,000 (Cell Signaling Technology); HRP–anti-sheep, 1:2,000 (Binding Site).

Statistics

Unpaired *t* tests were used for comparisons between age-matched control and *mIgf*$^{+/+}$, *mdx:mIgf*$^{+/+}$, and *mdx* muscles, and between *mdx* and *mdx:mIgf*$^{+/+}$ muscles. Statistical significance was accepted for comparisons where $P < 0.05$.

The authors thank C.A. Morris (University of Pennsylvania School of Medicine, Philadelphia, PA) for many helpful discussions.

This work was supported by grants to H.L. Sweeney from the National Institutes of Health (R01AR47292) and the Muscular Dystrophy Association. E.R. Barton was supported by a fellowship from the Muscular Dystrophy Association. N. Rosenthal was supported by a grant from the Muscular Dystrophy Association. A Musaro was supported by Telethon (Italy) (GP0098Y01).

Submitted: 14 August 2001
Revised: 5 February 2002
Accepted: 19 February 2002

References

Adams, G.R., and S.A. McCue. 1998. Localized infusion of IGF-I results in skeletal muscle hypertrophy in rats. *J. Appl. Physiol.* 84:1716–1722.

Alessi, D.R., and P. Cohen. 1998. Mechanism of activation and function of protein kinase B. *Curr. Opin. Genet. Dev.* 8:55–62.

Allen, R.E., S.M. Sheehan, R.G. Taylor, T.L. Kendall, and G.M. Rice. 1995. Hepatocyte growth factor activates quiescent skeletal muscle satellite cells in vitro. *J. Cell. Physiol.* 165:307–312.

Anderson, J.E., W.K. Ovalle, and B.H. Bressler. 1987. Electron microscopic and autoradiographic characterization of hindlimb muscle regeneration in the *mdx* mouse. *Anat. Rec.* 219:243–257.

Barton-Davis, E.R., D.I. Shoturma, A. Musaro, N. Rosenthal, and H.L. Sweeney. 1998. Viral mediated expression of insulin-like growth factor I blocks the aging-related loss of skeletal muscle function. *Proc. Natl. Acad. Sci. USA.* 95: 15603–15607.

Brooks, S.V., and J.A. Faulkner. 1988. Contractile properties of skeletal muscles from young, adult and aged mice. *J. Physiol.* 404:71–82.

Campbell, K.P. 1995. Three muscular dystrophies: loss of cytoskeleton-extracellular matrix linkage. *Cell.* 80:675–679.

Carnwath, J.W., and D.M. Shotton. 1987. Muscular dystrophy in the *mdx* mouse: histopathology of the soleus and extensor digitorum longus muscles. *J. Neurol. Sci.* 80:39–54.

Chakravarthy, M.V., T.W. Abraha, R.J. Schwartz, M.L. Fiorotto, and F.W. Booth. 2000a. Insulin-like growth factor-I extends in vitro replicative life span of skeletal muscle satellite cells by enhancing G1/S cell cycle progression via the activation of phosphatidylinositol 3′-kinase/Akt signaling pathway. *J. Biol. Chem.* 275:35942–35952.

Chakravarthy, M.V., B.S. Davis, and F.W. Booth. 2000b. IGF-I restores satellite cell proliferative potential in immobilized old skeletal muscle. *J. Appl. Physiol.* 89:1365–1379.

Coleman, M.E., F. DeMayo, K.C. Yin, H.M. Lee, R. Geske, C. Montgomery, and R.J. Schwartz. 1995. Myogenic vector expression of insulin-like growth factor I stimulates muscle cell differentiation and myofiber hypertrophy in transgenic mice. *J. Biol. Chem.* 270:12109–12116.

Coolican, S.A., D.S. Samuel, D.Z. Ewton, F.J. McWade, and J.R. Florini. 1997. The mitogenic and myogenic actions of insulin-like growth factors utilize distinct signaling pathways. *J. Biol. Chem.* 272:6653–6662.

Decary, S., V. Mouly, C.B. Hamida, A. Sautet, J.P. Barbet, and G.S. Butler-Browne. 1997. Replicative potential and telomere length in human skeletal muscle: implications for satellite cell-mediated gene therapy. *Hum. Gene Ther.* 8:1429–1438.

Decary, S., C.B. Hamida, V. Mouly, J.P. Barbet, F. Hentati, and G.S. Butler-Browne. 2000. Shorter telomeres in dystrophic muscle consistent with extensive regeneration in young children. *Neuromuscul. Disord.* 10:113–120.

Deconinck, A.E., J.A. Rafael, J.A. Skinner, S.C. Brown, A.C. Potter, L. Metzinger, D.J. Watt, J.G. Dickson, J.M. Tinsley, and K.E. Davies. 1997. Utrophin-dystrophin-deficient mice as a model for Duchenne muscular dystrophy. *Cell.* 90:717–727.

Delaughter, M.C., G.E. Taffet, M.L. Fiorotto, M.L. Entman, and R.J. Schwartz. 1999. Local insulin-like growth factor I expression induces physiologic, then pathologic, cardiac hypertrophy in transgenic mice. *FASEB J.* 13:1923–1929.

D'Ercole, A.J., A.D. Stile, and L.E. Underwood. 1984. Tissue concentrations of somatomedin C: further evidence for multiple sites of synthesis and paracrine or autocrine mechanisms of action. *Proc. Natl. Acad. Sci. USA.* 81: 935–939.

Desypris, G., and D.J. Parry. 1990. Relative efficacy of slow and fast α-motoneurons to reinnervate mouse soleus muscle. *Am. J. Physiol.* 258:C62–C70.

Engert, J.C., E.B. Berglund, and N. Rosenthal. 1996. Proliferation precedes differentiation in IGF-I–stimulated myogenesis. *J. Cell Biol.* 135:431–440.

Florini, J.R., D.Z. Ewton, and S.A. Coolican. 1996. Growth hormone and the insulin-like growth factor system in myogenesis. *Endocr. Rev.* 17:481–517.

Harley, C.B. 1997. Human ageing and telomeres. *Ciba Found. Symp.* 211:129–139.

Hartigan-O'Connor, D., and J.S. Chamberlain. 2000. Developments in gene therapy for muscular dytrophy. *Microsc. Res. Tech.* 48:223–238.

Lawlor, M.A., and P. Rotwein. 2000a. Coordinate control of muscle cell survival by distinct insulin-like growth factor–activated signaling pathways. *J. Cell Biol.* 151:1131–1140.

Lawlor, M.A., and P. Rotwein. 2000b. Insulin-like growth factor-mediated muscle cell survival: central roles for Akt and cyclin-dependent kinase inhibitor p21. *Mol. Cell. Biol.* 20:8983–8995.

Louboutin, J.P., V. Fichter-Gagnepain, E. Thaon, and M. Fardeau. 1993. Morphometric analysis of mdx diaphragm muscle fibres. Comparison with hindlimb muscles. *Neuromuscul. Disord.* 3:463–469.

Lynch, G.S., S.A. Cuffe, D.R. Plant, and P. Gregorevic. 2001. IGF-I treatment improves the functional properties of fast- and slow-twitch skeletal muscles from dystrophic mice. *Neuromuscul. Disord.* 11:260–268.

McPherron, A.C., A.M. Lawler, and S.J. Lee. 1997. Regulation of skeletal muscle mass in mice by a new TGF-beta superfamily member. *Nature.* 387:83–90.

Morrison, J., Q.L. Lu, C. Pastoret, T. Partridge, and G. Bou-Gharios. 2000. T-cell-dependent fibrosis in the *mdx* mouse. *Lab. Invest.* 80:881–891.

Musaro, A., and N. Rosenthal. 1999. Maturation of the myogenic program is induced by postmitotic expression of insulin-like growth factor I. *Mol. Cell. Biol.* 19:3115–3124.

Musaro, A., K. McCullagh, A. Paul, L. Houghton, G. Dobrowolny, M. Molinaro, E.R. Barton, H.L. Sweeney, and N. Rosenthal. 2001. Localized Igf-1 transgene expression sustains hypertrophy and regeneration in senescent skeletal muscle. *Nat. Genet.* 27:195–200.

Petley, T.D., K. Graff, W. Jiang, H. Yang, and J.R. Florini. 1999. Variation among cell types in the signaling pathways by which IGF-I stimulates specific cellular responses. *Horm. Metab. Res.* 31:70–76.

Prowse, K.R., and C.W. Greider. 1995. Developmental and tissue-specific regulation of mouse telomerase and telomere length. *Proc. Natl. Acad. Sci. USA.* 92:4818–4822.

Rando, T.A., M.-H. Disatnik, and L.Z.-H. Zhou. 2000. Rescue of dystrophin expression in *mdx* mouse muscle by RNA/DNA oligonucleotides. *Proc. Natl. Acad. Sci. USA.* 97:5363–5368.

Renganathan, M., M.L. Messi, and O. Delbono. 1998. Overexpression of IGF-1 exclusively in skeletal muscle prevents age-related decline in the number of dihydropyridine receptors. *J. Biol. Chem.* 273:28845–28851.

Russell-Jones, D.L., A.M. Umpleby, T.R. Hennessy, S.B. Bowes, F. Shojaee-Moradie, K.D. Hopkins, N.C. Jackson, J.M. Kelly, R.H. Jones, and P.H. Sönksen. 1994. Use of a leucine clamp to demonstrate the IGF-I actively stimulates protein synthesis in normal humans. *Am. J. Physiol.* 267:E591–E598.

Samuel, D.S., D.Z. Ewton, S.A. Coolican, T.D. Petley, F.J. McWade, and J.R. Florini. 1999. Raf-1 activation stimulates proliferation and inhibits IGF-

stimulated differentiation in L6A1 myoblasts. *Horm. Metab. Res.* 31:55–64.

Sandri, M., and U. Carraro. 1999. Apoptosis of skeletal muscles during development and disease. *Int. J. Biochem. Cell Biol.* 31:1373–1390.

Sandri, M., C. Minetti, M. Pedemonte, and U. Carraro. 1998. Apoptotic myonuclei in human Duchenne muscular dystrophy. *Lab. Invest.* 78:1005–1016.

Schiaffino, S., and G. Salviati. 1997. Molecular diversity of myofibrillar proteins: isoform analysis at the protein and mRNA level. *In* Methods in Muscle Biology. Vol. 52. C.P. Emerson, Jr., and H.L. Sweeney, editors. Academic Press, New York. 349–369.

Sheehan, S.M., and R.E. Allen. 1999. Skeletal muscle satellite cell proliferation in response to members of the fibroblast growth factor family and hepatocyte growth factor. *J. Cell. Physiol.* 181:499–506.

Shrager, J.B., A. Naji, A.M. Kelly, and H.H. Stedman. 1992. A PCR-based assay for the wild-type dystrophin gene transferred into the *mdx* mouse. *Muscle Nerve.* 15:1133–1137.

Sicinski, P., Y. Geng, A.S. Ryder-Cook, E.A. Barnard, M.G. Darlison, and P.J. Barnard. 1989. The molecular basis of muscular dystrophy in the *mdx* mouse: a point mutation. *Science.* 244:1578–1580.

Spencer, M.J., C.M. Walsh, K.A. Dorshkind, E.M. Rodriguez, and J.G. Tidball. 1997. Myonuclear apoptosis in dystrophic *mdx* muscle occurs by perforin-mediated cytotoxicity. *J. Clin. Invest.* 99:2745–2751.

Stedman, H.H., H.L. Sweeney, J.B. Shrager, H.C. Maguire, R.A. Panettieri, B. Petrof, M. Narusawa, J.M. Leferovich, J.T. Sladky, and A.M. Kelly. 1991. The *mdx* mouse diaphragm reproduces the degenerative changes of Duchenne muscular dystrophy. *Nature.* 352:536–539.

Straub, V., J.A. Rafael, J.S. Chamberlain, and K.P. Campbell. 1997. Animal models for muscular dystrophy show different patterns of sarcolemmal disruption. *J. Cell Biol.* 139:375–385.

Thomas, M., B. Langley, C. Berry, M. Sharma, S. Kirk, J. Bass, and R. Kambadur. 2000. Myostatin, a negative regulator of muscle growth, functions by inhibiting myoblast proliferation. *J. Biol. Chem.* 275:40235–40243.

Vandromme, M., A. Rochat, R. Meier, G. Carnac, D. Besser, B.A. Hemmings, A. Fernandez, and N.J. Lamb. 2001. Protein kinase B beta/Akt2 plays a specific role in muscle differentiation. *J. Biol. Chem.* 276:8173–8179.

Wang, B., L. Juan, and X. Xiao. 2000. Adeno-associated virus vector carrying human minidystrophin genes effectively ameliorates muscular dystrophy in *mdx* mouse model. *Proc. Natl. Acad. Sci. USA.* 97:13714–13719.

Wright, W.E., and J.W. Shay. 2000. Telomere dynamics in cancer progression and prevention: fundamental differences in human and mouse telomere biology. *Nat. Med.* 6:849–851.

Wu, W., W.L. Lee, Y.Y. Wu, D. Chen, T.J. Liu, A. Jang, P.M. Sharma, and P.H. Wang. 2000. Expression of constitutively active phosphatidylinositol 3-kinase inhibits activation of caspase 3 and apoptosis of cardiac muscle cells. *J. Biol. Chem.* 275:40113–40119.